



Published in final edited form as:

*J Immunol.* 2017 August 01; 199(3): 931–940. doi:10.4049/jimmunol.1700348.

## B cells produce type 1 interferons in response to the Toll-like receptor 9 agonist CpG-A conjugated to cationic lipids

Munir Akkaya<sup>1,\*</sup>, Billur Akkaya<sup>2</sup>, Pietro Miozzo<sup>1,\*\*</sup>, Mukul Rawat<sup>3</sup>, Mirna Pena<sup>1</sup>, Patrick W. Sheehan<sup>1</sup>, Ann S. Kim<sup>1,\*\*\*</sup>, Olena Kamenyeva<sup>4</sup>, Juraj Kabat<sup>4</sup>, Silvia Bolland<sup>1</sup>, Akanksha Chaturvedi<sup>3</sup>, and Susan K. Pierce<sup>1,\*</sup>

<sup>1</sup>Laboratory of Immunogenetics, National Institute of Allergy and Infectious Diseases, National Institutes of Health, Rockville, MD 20852, USA

<sup>2</sup>Laboratory of Immunology, National Institute of Allergy and Infectious Diseases, National Institutes of Health, Bethesda, MD 20892, USA

<sup>3</sup>Indian Institute of Science Education and Research (IISER), Pune 411 008, India

<sup>4</sup>Biological Imaging Facility, National Institute of Allergy and Infectious Diseases, National Institutes of Health, Bethesda, MD 20892, USA

### Abstract

B cells express the innate receptor, toll-like receptor 9 (TLR9), which signals in response to unmethylated CpG sequences in microbial DNA. Of the two major classes of CpG-containing oligonucleotides, CpG-A appears restricted to inducing type 1 interferon (type 1 IFN) in innate immune cells and CpG-B to activating B cells to proliferate and produce antibodies and inflammatory cytokines. Although CpGs are candidates for adjuvants to boost innate and adaptive immunity, our understanding of the effect of CpG-A and CpG-B on B cell responses is incomplete. Here we show that both CpG-B and CpG-A activated B cells *in vitro* to proliferate, secrete antibodies and IL-6 and that neither CpG-B nor CpG-A alone induced type 1 IFN production. However, when incorporated into the cationic lipid, DOTAP, CpG-A, but not CpG-B induced a type 1 IFN response in B cells *in vitro* and *in vivo*. We provide evidence that differences in the function of CpG-A and CpG-B may be related to their intracellular trafficking in B cells. These findings fill an important gap in our understanding of the B cell response to CpGs with implications for the use of CpG-A and CpG-B as immunomodulators.

### Keywords

CpG; TLR 9; B cells; DOTAP; Interferon

\* Address correspondence to Susan K. Pierce (spierce@nih.gov), and Munir Akkaya (munir.akkaya@nih.gov), NIH/NIAID/LIG, 12441 Parklawn Drive, Rockville, MD 20852, USA. Phone: (301) 480-3875; Fax: (301) 402-0259.

\*\* Current Address: University of Massachusetts Medical School, Worcester, MA 01655

\*\*\* Current Address: Cleveland Clinic Lerner College of Medicine, Cleveland, OH 44195

### Author Contributions

MA, SKP conceived the project. SKP secured the funding. MA, BA, AC, PM, MR, PWS, ASK, OK performed the experiments. MA, BA, AC, OK, JK, CQ, SB, SKP analyzed the data. MP provided technical help, MA wrote the manuscript, SKP edited the manuscript.

### Conflict of Interest

The authors declare no conflicts of interests.

## Introduction

TLR9 is a pattern recognition receptor that senses unmethylated CpG sequences in microbial DNA (1, 2). TLR9 is expressed intracellularly in a wide variety of immune cells and is a strong stimulator of innate immunity in response to pathogens (3). In addition to cells of the innate immune system, TLR9 is expressed in B cells and is a potent activator of B cells (4) in addition to its ability to alter the outcome of B cell receptor (BCR) signaling (5, 6).

Synthetic analogs of microbial CpG sequences have been developed both to optimize the immune cell activating potential of CpGs as adjuvants and to increase their selectivity for particular immune cell types (7–9). These oligodeoxynucleotides (ODNs) are generally 15–20 deoxynucleotides in length and contain one or more CpG sequences. Many of these ODNs are reinforced with nuclease-resistant phosphorothioate bonds, which at least partially replace the relatively fragile phosphodiester bonds to improve their stability *in vitro* and *in vivo*. Of the varieties of ODNs, CpG-A and CpG-B are among the most commonly used. CpG-A ODNs generally contain only one CpG sequence and a poly-G sequence in their 3' end and are partially phosphorothioate reinforced. CpG-A ODNs form 3D hairpin structures and are poorly soluble in salt solutions (3, 10). In contrast, CpG-B ODNs are fully phosphorothioate reinforced, highly soluble linear structures that contain multiple CpG sequences but no poly-G sequences (10, 11). Although both CpG-A and CpG-B activate TLR9, the two CpG-containing ODNs elicit different responses. CpG-A induces robust IRF7-dependent type 1 IFN responses in plasmacytoid dendritic cells (pDCs). Conversely, CpG-B is ineffectual in inducing type 1 IFN in pDCs but readily activates B cells in an NF- $\kappa$ B-dependent fashion to proliferate and differentiate into Ab-producing cells and to secrete proinflammatory cytokines. At present we do not have a full understanding of the B cell response to CpG-A in terms of the ability of CpG-A to activate NF- $\kappa$ B dependent responses in B cells and whether CpG-A under any circumstances is able to induce type 1 IFN responses. This is a critical gap in knowledge that could potentially impact the development of CpG-A as an immunomodulator *in vivo*.

To more fully understand the effects of CpG-A and CpG-B on B cell function, we carried out a detailed analysis of the B cell response to CpG-A and CpG-B alone and to CpG-A and CpG-B conjugated with the cationic carrier, DOTAP, that was shown to improve the uptake (12) and the intracellular trafficking of CpGs-ODNs in various cell types (13). We provide evidence that as compared to CpG-A, CpG-B induces responses that are more rapid and of greater magnitude including proliferation, Ab secretion and proinflammatory cytokine production. However, CpG-A was equivalent to CpG-B in its effect on the expression of a variety of B cell surface markers. Neither CpG-A nor CpG-B alone induced detectable production of type 1 IFN whereas treatment with CpG-A-DOTAP, but not CpG-B-DOTAP, resulted in type 1 IFN transcription and secretion *in vitro* and *in vivo*. We provide evidence that differences in their intracellular trafficking in B cells may contribute to the different functional outcomes of CpG-A-DOTAP and CpG-B-DOTAP treatment. Taken together, these data provide a more complex picture of the effects of CpG-A and CpG-B on B cell responses than formerly appreciated and have important implications for their use.

## Materials and Methods

### Animals and reagents

WT (C57BL/6), IFN- $\beta$ 1 YFP reporter (14) (B6.129-*Ifnb1<sup>tm1Lky</sup>/J*), Myd88 KO mice (*B6.129P2(SJL)-Myd88tm1.1Defr/J*) and B cell deficient (15) (B6.129S2-Ighmtm1Cgn/J: MuMT) mice were purchased from Jackson Laboratory (Bar Harbor, ME, USA). TLR9 KO mice in C57BL/6 background (1) were kindly provided by Cristiana Guiducci [Dynavax Technologies, Berkeley, CA, USA]. All mice were maintained at the National Institutes of Health animal facilities in compliance with Animal Care and Use Committee standards.

Cells were cultured in sterile complete RPMI media (RPMI 1640 medium supplemented with 50 U/ml penicillin, 50  $\mu$ M streptomycin, 10% heat-inactivated fetal calf serum, 2 mM L-glutamine, 1 mM sodium pyruvate, 0.1 mM non-essential amino acids, 50  $\mu$ M  $\beta$ -mercaptoethanol and 10 mM HEPES) (ThermoFisher, Waltham, MA, USA). For magnetic separations, cells were maintained in filtered and degassed MACS buffer: PBS (Lonza, Allendale, NJ, USA) supplemented with 0.5% BSA (Sigma-Aldrich, St. Louis, MO, USA) and 2 mM EDTA (Sigma-Aldrich). Samples were stained for flow cytometry in FACS buffer (HBSS supplemented with, 1% HEPES, 2% FCS and 10mM Sodium Azide (Sigma-Aldrich) using antibodies listed in Supplementary Table 1.

### Purification of B cells and pDCs

Mice were euthanized by CO<sub>2</sub> asphyxiation and spleens were removed. B cells were purified using a mouse B cell isolation kit (Miltenyi Biotec, San Diego, CA, USA) as previously described in (16). For IFN ELISA experiments high purity pDCs were obtained from mouse spleen using a mouse plasmacytoid dendritic cell isolation kit (Miltenyi Biotec). For flow cytometry-based experiments, pDCs were differentiated from mouse bone marrow cells. For this purpose, using sterile equipment, femurs and tibias of euthanized IFN- $\beta$ 1 YFP reporter mice were harvested. Upon removal of muscles and connective tissues surrounding the bone, top portions of metaphyses were cut out on both sides to expose the medullary cavity. Using a syringe and a needle, the medullary cavity was flushed with sterile PBS. Single cell suspension was obtained by mashing the clumps and then filtering through 70  $\mu$ m cell strainers (Corning Inc., Vienna, VA, USA). Cells were centrifuged and the pellet was resuspended in complete RPMI supplemented with 200ng/ml Flt-3L (eBioscience, San Diego, CA, USA). Cell suspensions (at a density of approximately  $1-2 \times 10^6$  cells/ml) were plated into sterile 6-well tissue culture plates (Corning) (2ml/well). Plates were incubated in a 37°C 5% CO<sub>2</sub> incubator. On day 4, 1 ml of the culture media was replaced with fresh Flt3L supplemented media. On day 8, supernatants were discarded and loosely plate bound pDCs were harvested by pipetting.

### In vitro cellular assays

B cells ( $2.5 \times 10^5$ ) were plated into sterile 96 well round bottom plates (Corning) in complete RPMI media. Treatment of cells with CpG-A and CpG-B was carried out using ODN1585 and ODN1826 respectively. CpG ODNs and their negative controls, containing GpC instead of CpG, were purchased from Invivogen (San Diego, CA, USA). For conditions involving cationic lipid-ODN complexes, N-[1-(2,3-Dioleoyloxy)propyl]-N,N,N-

trimethylammonium methyl-sulfate (DOTAP), a cationic lipid based liposomal transfection reagent (Roche, Basel, Switzerland) was used. For this purpose, ODNs and DOTAP were added into HBS (Sigma-Aldrich, St. Louis, MO, USA) in separate tubes at the desired amounts. These solutions were mixed without agitation and the resulting DOTAP-ODN mixture was incubated at RT for 15–20 minutes before being added to the culture media.

### Quantitative RT-PCR (qPCR) and PCR arrays

RNA was isolated from *in vitro* stimulated B cells using either RNeasy mini or RNeasy micro kits (Qiagen, Hilden, Germany) following the manufacturer's instructions. For qPCR and PCR array experiments, cDNA was generated using iScript™ Reverse Transcription Supermix (Bio Rad, Hercules, CA, USA) and RT2 reverse transcription kit (Qiagen) respectively. For qPCR, amplification of the target genes was carried out using specific primers and Taqman probes, listed in Supplementary Table 1 (Integrated DNA Technologies, Coralville, IA, USA) and Platinum® Quantitative PCR SuperMix-UDG (ThermoFisher). Analysis of the fold change in gene expression between stimulated and control groups was carried out using the delta delta CT method, described previously (17).

For PCR amplification of multiple IFN response genes, RT<sup>2</sup> SYBR® Green qPCR Mastermix was used together with RT<sup>2</sup> Profiler™ PCR Array (PAMM-016ZD-2) (Qiagen). Data analysis was carried out using the software provided on the manufacturer's website.

### Injections

Intravenous injections of mice were performed through tail veins using 200 µl/ mouse sterile HBS solution, containing ODNs (conjugated with DOTAP or unconjugated).

### ELISAs

Levels of cytokines (IL-6, IFN- $\alpha$ , IFN- $\beta$ ) and immunoglobulins (IgM) secreted in response to stimulation of B cells *in vitro* were measured from supernatants using Ready Set Go mouse IL-6 (eBioscience) ELISA, Platinum mouse IFN- $\alpha$  ELISA (eBioscience), Verikine Mouse IFN- $\beta$  ELISA (PBL Assay Science, Piscataway, NJ, USA) and Ready Set Go mouse IgM ELISA (eBioscience) respectively. Serum levels of IFN- $\alpha$  and  $\beta$  were measured using diluted serum of the ODN injected mice and the relevant ELISA kits.

### Confocal microscopy

Purified B cells were attached onto Poly-L Lysine coated coverslips and stimulated at 37 °C with media containing fluorescently labeled ODNs (Solulink, San Diego, USA) either alone or in conjugation with DOTAP. Co-localization of internalized ODNs with LysoTracker green (a lysosomal sensor) (ThermoFisher) was traced by live imaging using LSM 710 confocal microscopy (Zeiss, Oberkochen, Germany). Approximately 30 cells that were positive for both LysoTracker and CpG were analyzed by Zen blue (Zeiss, Germany) and Manders colocalization coefficients of fluorescently labeled CpGA or CpGB with LysoTracker green were calculated.

## Live Imaging of Tissue Sections

Spleens of IFN- $\beta$  YFP mice previously injected with i.v. DOTAP-ODN complexes were harvested and kept on ice in PBS supplemented with 1% BSA. Preheated RPMI-2% Agarose (Lonza) was chilled to 38°C and then poured onto spleens in petri dishes on ice. Upon polymerization of agarose, phenol red-free complete RPMI media was added. Using a VT1000S vibrating blade microtome (Leica, Wetzlar, Germany) 300–350  $\mu$ m thick slices were obtained with minimal disruption to tissue architecture. Sections were incubated in complete RPMI media at 37 °C, in a 5%CO<sub>2</sub> incubator for 2h. Then sections were stained with fluorochrome labeled CD4, B220 and CD11c antibodies and held down using tissue anchors (Warner Instruments, Hamden, CT,USA) in 14 mm microwell dishes (MatTek, Ashland, MA, USA). Confocal microscopy imaging was carried out using a Leica SP8 inverted 5 channel confocal microscope equipped with an Environmental Chamber as previously described (18). Images were analyzed using Imaris Software (Bitplane, Zurich, Switzerland).

## Barcoding and flow cytometry

Phospho-flow experiments were carried out using the barcoding strategy described previously (19). Briefly, cells were stimulated for indicated durations using CpG-A or CpG-B, fixed, permeabilized and barcoded with different fluorochrome conjugates of B220 and CD45 antibodies. The resulting 12 barcoded samples were washed, pooled and stained as one with antibodies against phosphorylated kinases.

Surface expression of various proteins was also screened using a similar strategy. For this purpose B cells, stimulated for 24 hours, were harvested, stained with a live-dead marker and barcoded using a combination of fluorochrome-labeled B220 and CD45 antibodies. The resulting barcoded samples were combined and stained with PE conjugated markers of interest.

Flow cytometry experiments were carried out using BD LSR-II Cytometer and data were analyzed in FlowJo software.

## Statistical analyses

Statistical analyses were carried out in Graphpad Prism software. Student's T test was used to determine the significance of the difference observed. ( $P > 0.05 = \text{ns}$ ;  $0.01 < P < 0.05 = *$ ;  $0.001 < P < 0.01 = **$ ;  $0.0001 < P < 0.001 = ***$ ;  $P < 0.0001 = ****$ ).

## Results

### Induction of Akt and p38 phosphorylation by CpG-B and CpG-A

TLR9 ligation triggers signaling cascades in B cells that result in the phosphorylation of several cytoplasmic kinases, including p38 (MAPK) and Akt (20, 21). We compared the ability of CpG-A and CpG-B alone to activate TLR9 to signal for phosphorylation of these kinases. B cells were purified from mouse spleens by negative selection using a Miltenyi Biotec mouse B cell isolation kit and were incubated with 1  $\mu$ M CpG-A or CpG-B for increasing lengths of time up to 90 min. The cells were harvested, fixed, permeabilized,

barcoded using combinations of B220-specific Abs labeled with three different fluorophores to uniquely label six B cell samples as recently described (19) and stained with FL-conjugated Abs specific for phospho-Akt or phospho-p38. Both CpG-A and CpG-B treatment induced B cells to phosphorylate Akt and p38, detectable at the first time point, 15 min after treatment. However, B cells treated with CpG-B were induced to phosphorylate both Akt and p38 more rapidly and at levels significantly higher than B cells treated with CpG-A (Figure 1A, B and Supplementary Figure 1A). This was the case even when compared to B cells treated with CpG-A at a higher concentration, namely 5  $\mu$ M (data not shown). Thus, for the activation of TLR9 signaling in B cells CpG-B is considerably more effective than CpG-A.

### **The TLR9-dependent stimulation of B cell proliferation, Ab secretion and proinflammatory cytokine secretion by CpG-A and CpG-B**

TLR9 induces NF- $\kappa$ B mediated increases in B cell proliferation and antibody secretion as well as secretion of proinflammatory cytokines (4). B cells, both wild type (WT) and TLR9-deficient (TLR9 KO) were stained with an e450-labeled proliferation dye and incubated with CpG-A or CpG-B at increasing concentrations (up to 10  $\mu$ M) for 48 h. CpG-B induced proliferation in over 90% of B cells that was maximal at a concentration of 1  $\mu$ M CpG-B (Figure 1C and Supplementary Figure 1B). CpG-A also induced a proliferative response but as compared to CpG-B the response was weaker, activating only 50% of cells at 10  $\mu$ M. For both CpG-A and CpG-B the proliferative responses were TLR9-dependent (Figure 1C).

To assess CpG-induced Ab secretion, B cells were incubated with 2  $\mu$ M CpG-A or CpG-B, culture supernatants collected daily for seven days and the IgM in the supernatants quantified by ELISA. The viability of the B cells was comparable for CpG-A and CpG-B stimulated cells over the course of the experiment and in both cases, higher than unstimulated cells (Supplementary Figure 1C). CpG-B treatment resulted in production of IgM that was detectable earlier (day 2 versus day 3) reached approximately three fold higher levels of IgM (maximally  $0.5 \times 10^4$  ng/ml versus  $1.5 \times 10^4$  ng/ml) as compared to CpG-A-treated B cells (Figure 1D). For both CpG-A and CpG-B, IgM secretion was TLR9-dependent.

When activated through TLR9, B cells produce the proinflammatory cytokine IL-6 in an NF- $\kappa$ B dependent fashion (22). To determine the effect of CpG-A and CpG-B on the synthesis and secretion of IL-6, B cells were treated with 5  $\mu$ M CpG-A or CpG-B for 90 min and the fold change in IL-6 mRNA expression was determined. Although treatment with either CpG-A or CpG-B resulted in increases in IL-6 gene transcription, the effect of CpG-B was 3–4 fold higher as compared to that of CpG-A (Figure 1E). In a separate experiment, B cells purified from WT or TLR9 KO mice were treated with increasing concentrations of CpG-A or CpG-B and after an 18 h incubation, supernatants were collected and IL-6 levels were measured by ELISA. Treatment with CpG-B induced maximal secretion of IL-6 (in the  $\mu$ g/ml range) at concentrations of CpG-B less than 1  $\mu$ M (Figure 1F). CpG-A induced similar levels of IL-6 (approximately .75  $\mu$ g/ml) but only at a CpG-A concentration of 10  $\mu$ M. Even at these relatively high concentrations of CpG-A, IL-6 secretion did not appear to be maximal. Importantly, the effect of both CpG-A and CpG-B on B cell IL-6 secretion was

TLR9-dependent (Figure 1F). Taken together these results indicate that CpG-A induces qualitatively similar TLR9-dependent responses to that of CpG-B albeit it at quantitatively reduced levels.

To determine if CpG-A treatment induced B cells to produce type 1 IFNs, purified B cells were treated for 18 h with 5  $\mu$ M CpG-A or CpG-B, the supernatants were collected and the amount of IFN- $\beta$  present in the supernatants was quantified by ELISA. In the same experiment, pDCs purified from spleen were treated with CpG-A as a positive control. Neither CpG-A nor CpG-B treatment induced detectable IFN- $\beta$  secretion from B cells. In contrast, pDCs produced IFN- $\beta$  (over 100 pg/ml) in response to CpG-A treatment (Figure 1G).

We also tested the ability of CpG-A and CpG-B to alter the cell surface expression of approximately 40 B cell surface proteins that were affected by CpG-B treatment based on the preliminary results of a screen for the expression of approximately 250 mouse surface proteins using a BioLegend LEGENDScreen kit. Purified B cells were cultured in media alone or in media containing CpG-A or CpG-B (2  $\mu$ M) for 24 h. Cells were barcoded, pooled and stained with a panel of PE-conjugated Abs specific for the surface markers shown in Figures 1H, I. For the most part the effect of CpG-A and CpG-B on the B cells' expression of surface markers followed a similar pattern in that treatment either increased or decreased expression of any given marker. However, the magnitude of the effect was not equivalent for each marker. For example the expression of CD69, a cell activation marker, increased eight-fold in response to CpG-B but only two-fold in response in CpG-A, possibly reflecting the overall weaker induction of TLR9 signaling in B cells by CpG-A as compared to CpG-B. However, CpG-A induced similar increases to that of CpG-B in the expression of several markers including CD86, a key co-stimulatory molecule that plays a major role in B cell-T cell interaction (23) and MHC-Class-II (detected by IA/IE mAb). The expression of CD83, another activation marker playing role in B cell-T cell interaction (24) and PD-1, a well-known immune regulator (25) was increased to higher levels by CpG-A treatment compared to CpG-B treatment. CpG-A and CpG-B treatment had similar effects in decreasing the expression of a subset of markers including the integrins, LPAM-1 and PIR-A/B.

### **Conjugation of CpG-A and CpG-B to cationic lipids alters the outcome of B cell responses to CpG treatment in vitro**

The conjugation of CpG-containing ODNs to carriers, in particular cationic lipids, has been shown to alter the uptake and (12) trafficking of CpG containing-ODNs (13) As a consequence, the compartments in which the CpG-containing ODNs encounter and activate TLR9 can be altered as can the outcomes of TLR9 signaling in terms of the cytokines secreted. We analyzed the effect of conjugation of CpG-A and CpG-B to the cationic lipid based transfection reagent, DOTAP, on the outcome of TLR9 signaling in B cells. We first monitored the intracellular trafficking of Cy3-conjugated CpG-A and Cy5-CpG-B alone or conjugated to DOTAP into late endosomal/lysosomal compartments by confocal microscopy using LysoTracker to mark late acidic compartments. Purified mouse B cells were incubated with Cy3-CpG-A alone or Cy5-CpG-B alone or their DOTAP conjugates (1 $\mu$ M CpG at a

ratio of 1 CpG:3 DOTAP) for increasing lengths of time up to 180 min. Twenty minutes before the end of each incubation the cells were placed in poly-L-Lysine coated chamber wells and incubated with LysoTracker (75nM) at 37°C, washed and confocal images were acquired and the colocalization of the CpG-A and CpG-B with LysoTracker was quantified. Shown are representative images for Cy-3-CpG-A and Cy-5-CpG-B alone or conjugated with DOTAP and LysoTracker at the 60 and 180 min time points (Figure 2A). The quantification of colocalization of Cy3-CpG-A and Cy5-CpG-B alone or conjugated with DOTAP with LysoTracker for the 30, 60 and 180 min time points are also given (Figure 2B). The colocalization of CpG-A alone with LysoTracker was significantly less than that of CpG-B alone at all time points indicating that CpG-A is retained in less acidic compartments as compared to CpG-B that accumulated in late endosomes/lysosomes. The conjugation of CpG-A to DOTAP had little effect on its colocalization with LysoTracker with CpG-A-DOTAP showing only a small increase in its colocalization with LysoTracker as compared to CpG-A alone at the 180 min time point. Thus, both CpG-A and CpG-A-DOTAP accumulate in intracellular compartments that are not stained by LysoTracker. However, because considerable heterogeneity may exist in these early, less acidic endosomal compartments that would not be revealed using LysoTracker, we leave open the possibility that conjugation to DOTAP resulted in the concentration of CpG-A in compartments separate from those to which unconjugated CpG-A localized. The accumulation of CpG-B-DOTAP in LysoTracker-containing compartments was significantly increased at the 60 min and 180 min time points as compared to CpG-B alone. It is not clear whether DOTAP facilitated the trafficking of CpG-B to late endosomes/lysosomes or if DOTAP enhanced the accumulation of CpG-B in acidic compartments by either blocking the degradation of CpG-B or its clearance from these compartments. Taken together these results indicate that CpG-B and CpG-B-DOTAP trafficked to late endosomal/lysosomal acidic compartments whereas CpG-A and CpG-A-DOTAP were retained in LysoTracker-negative compartments. The rapid movement of CpG-B to late endosome/lysosome compartments and the retention of CpG-A in early endosomes may contribute, in part, to the more efficient stimulation of B cells to proliferate and secrete cytokines and Abs by CpG-B as compared to CpG-A.

To determine if conjugating DOTAP to CpG-ODNs altered the outcome of TLR9 signaling in B cells, purified mouse splenic B cells were incubated with CpG-A, CpG-B or their DOTAP conjugates, and harvested 90 min later and changes in the transcription of genes encoding type-1 IFNs were quantified by RT-PCR. Significant increases in the transcriptions of IFN- $\alpha$ 2, IFN- $\alpha$ 4, IFN- $\alpha$ 5 and IFN- $\beta$ 1 were observed but only for B cells treated with CpG-A-DOTAP (at a ratio of 1 CpG:3 DOTAP) (Figure 3A). In separate experiments B cells were treated for 18h with DOTAP alone, CpG-A-DOTAP or CpG-B-DOTAP and the amount of IFN- $\beta$ 1 in the culture supernatant quantified by ELISA. Only treatment with CpG-A-DOTAP resulted in secretion of IFN- $\beta$ 1 (Figure 3B). Thus, conjugation of CpG-A but not CpG-B to DOTAP dramatically altered the outcome of signaling, inducing type 1 IFN in B cells. Although both CpG-A and CpG-A-DOTAP accumulated in LysoTracker-negative compartments, the differential response of B cells to CpG-A versus CpG-A-DOTAP suggests the possibility that CpG-A and CpG-A-DOTAP may accumulate in qualitatively different endosomal compartments that would not be revealed by LysoTracker. Alternatively,



CpG-A and CpG-A-DOTAP may accumulate in the same compartments but interact with TLR9 in a qualitatively different fashion.

The cells used in these experiments were over 99.3% CD19<sup>+</sup> B cells. Nonetheless, it is possible that a small number of contaminating DCs or macrophages contributed to the observed increases in type 1 IFN transcription and secretion in CpG-A-DOTAP treated B cell cultures. To verify that B cells produced type 1 IFN when treated with CpG-A-DOTAP, we used a type 1 IFN-reporter mouse in which the *Irf1* gene was targeted to introduce an IRES and yellow fluorescent protein (YFP) immediately behind the stop codon of the gene (IFN- $\beta$  YFP mice) (14). When the *Irf1* gene is activated, YFP is co-translated such that cells that express IFN- $\beta$  can be detected by flow cytometry. Plasmacytoid DCs have been shown to produce type 1 IFN in response to CpG-A, CpG-A-DOTAP or CpG-B-DOTAP but not to CpG-B alone (13). To verify this observation in the mouse model, pDCs that were generated from bone marrow cells of the IFN- $\beta$ -YFP mice were treated with 5  $\mu$ M CpG-A or CpG-B or control ODNs (in which the CpG motif was replaced by GpC) with or without DOTAP for 18 h and the YFP fluorescence was quantified by flow cytometry in pDCs, gating on CD11c<sup>+</sup> PDCA1<sup>+</sup> B220<sup>+</sup> cells (Supplementary Figure 2). Both CpG-A and CpG-A-DOTAP treatment resulted in similar increases in YFP fluorescence in pDCs (Figure 3C). In contrast, pDCs produced very little YFP in response to CpG-B alone but responded to CpG-B-DOTAP (Figure 3C) consistent with previous reports (13). The pDCs did not respond to the control CpG-A or CpG-B.

B cells purified from spleens of IFN- $\beta$ -YFP mice were treated as above and YFP fluorescence was quantified in B cells by flow cytometry, gating on CD19<sup>+</sup> B220<sup>+</sup> cells. Treatment with CpG-A-DOTAP but not with CpG-A alone or CpG-B alone or CpG-B-DOTAP resulted in increased YFP expression in B cell (Figure 3D). Of interest, in approximately 6% of B cells treated with DOTAP conjugated to the CpG-A control (GpC) ODN, but not with DOTAP alone, produced YFP indicating that TLR9 independent pathways may contribute to the induction of type 1 IFN in B cells. To test this possibility, B cells isolated from WT and TLR9 KO mice were treated with CpG-A-DOTAP for 90 min and the mRNA levels encoding type 1 IFNs were quantified. Although increases in type 1 IFN gene expression were observed in both WT and TLR9 KO B cells, the increase in WT B cells were approximately five fold higher than those observed in TLR9 KO (Figure 3E), confirming the involvement of both TLR9-dependent and -independent pathways in CpG-A-DOTAP induced type 1 IFN synthesis.

We also tested the effect of conjugating DOTAP to CpG-A and CpG-B on the induction of IL-6 secretion by B cells. Purified B cells were treated *in vitro* with CpG-A or CpG-B (1 or 5  $\mu$ M) or with CpG-A-DOTAP or CpG-B-DOTAP and IL-6 in the supernatants was quantified by ELISA 18h later. We observed no effect of conjugation of DOTAP to either CpG-A or CpG-B on their ability to stimulate B cells to secrete IL-6 (Figure 3F). CpG-A and its DOTAP conjugate induced low levels of IL-6 secretion as compared to the high levels of IL-6 secreted by B cells in response to either CpG-B alone or CpG-B-DOTAP.

To gain a broader view of the effect of treatment of CpG-A and CpG-B and their DOTAP conjugates on B cell responses we compared the expression of a set of genes that are related

to the production of or response to either pro-inflammatory cytokines or type 1 IFNs. Purified B cells were treated with CpG-A or CpG-B (2  $\mu$ M) either alone or conjugated to DOTAP, mRNA was extracted and analyzed by q-PCR and the data were displayed as a heat map showing the expression of the genes in stimulated cells as compared to the unstimulated B cell control (Fig. 3G). Unexpectedly, a number of genes involved in type 1 IFN expression were upregulated in CpG-A treated B cells as compared to unstimulated B cells including the transcription factors Irf-1, -2 and -7 (26) and Ifih1 (MDA-5) and Ddx58, cytosolic sensors that respond to double stranded RNA and induce type 1 IFN responses (27) as well as genes that regulate the response to type 1 IFN including Ifit-1, -2 and 3; Mx-1 and 2, Oas1 and 2 (28). The expression of several of these genes was upregulated further in B cells treated with CpG-A-DOTAP. Thus, even though we were unable to detect type 1 IFN expression or secretion in CpG-A treated B cells (Fig. 3A,B) these results indicate that B cells were stimulated by CpG-A alone to make a type 1 IFN response signature. Consistent with the results in Fig. 3A,B expression of *Ifnb1* was only detected in CpG-A-DOTAP treated B cells but not in B cells treated with CpG-A alone. This analysis also showed that CpG-B and CpG-B-DOTAP treated B cells not only fail to produce type 1 IFN but may down regulate the IFN associated genes that are upregulated in CpG-A and CpG-A-DOTAP treated B cells. For most of these genes the effect is relatively modest but more pronounced for *Ifit1*, 2, and 3. Thus, triggering NF- $\kappa$ B-dependent pathways in B cells by CpG-B appears to have the potential to down regulate the expression of type 1 IFN associated genes.

### The effects of CpG-A-DOTAP on type 1 IFN responses in vivo

To assess the effect of CpG-A-DOTAP on the expression of type 1 IFN by B cells *in vivo*, IFN- $\beta$ -YFP mice were injected intravenously with CpG-A-DOTAP at different conjugation ratios of DOTAP and CpG-A or DOTAP alone. Mice were euthanized and spleens were collected 18h later. Splenocytes were stained with Abs specific for the B cell markers CD19 and B220 and YFP expression in the B cell gate (CD19<sup>+</sup> B220<sup>+</sup>) was quantified by flow cytometry (Figure 4A). B cells from mice treated with CpG-DOTAP at all three conjugation ratios resulted in approximately 2% of total B cells expressing YFP as compared to less than 1% of B cells from mice that received DOTAP alone. Mice injected with CpG-A alone did not generate YFP<sup>+</sup> B cells (data not shown) In addition, using antibodies to discriminate major splenic B cell subsets (marginal zone, follicular and transitional B cells) we showed no significant difference in the responsiveness of these subsets to CpG-A DOTAP stimulation *in vivo* (data not shown).

Although activation of B cells by CpG-A-DOTAP *in vivo* is less efficient than *in vitro* in that the percent of B cells activated to express type 1 IFN following administration of CpG-A-DOTAP *in vivo* (2%) is less than that activated *in vitro* (17%), these data clearly provide evidence that CpG-A-DOTAP functions *in vivo*. We also imaged YFP-expressing cells in intact spleen sections. IFN- $\beta$ -YFP mice given CpG-A or DOTAP alone or CpG-A-DOTAP intravenously were euthanized 3, 10 or 18 h post treatment and freshly prepared spleen sections were stained with fluorochrome conjugated Abs specific for CD4, CD11c or B220. By confocal microscopy, YFP-expressing cells were only detected in the spleens of mice that received CpG-A-DOTAP beginning 10 h post treatment (Figure 4B). The number of YFP-expressing cells per mm<sup>3</sup> in spleen sections were quantified (Fig. 4C). In 3D

reconstructions of multiple Z-stacks, we frequently observed YFP-expressing B cells (B220<sup>+</sup> CD11c<sup>-</sup> CD4<sup>-</sup>) (Figure 4D). However, it was not possible to quantify the frequency of YFP-expressing B cells in the three 3D reconstructions using the currently available image analysis tools due to the imprecise co-localization of the cytosolic YFP and B cell membrane markers.

We assessed the contribution of B cells to the overall IFN response to CpG-A-DOTAP by comparing IFN- $\beta$  levels in the serum of WT mice and B cell-deficient (muMT) mice three to 24 h after treatment with CpG-A-DOTAP. The serum levels of IFN- $\beta$  were significantly lower in the muMT mice as compared to WT mice (Figure 4E). Mice injected with CpG or DOTAP alone did not have detectable IFN- $\beta$  in their serum at these time points (data not shown). Taken together these results provide evidence that in response to CpG-A-DOTAP B cells contribute to the type 1 IFN response *in vivo* either directly or indirectly.

## Discussion

Here we report the results of a comprehensive analysis of the B cell response *in vitro* and to the TLR9 ligands CpG-A and CpG-B alone and conjugated to the cationic lipid carrier DOTAP. These results provide evidence for formerly unappreciated functions of CpG-A and CpG-B and insights as to how B cells might contribute to the overall immune response when these synthetic ODNs are administered systemically in various clinical settings.

Consistent with the published studies (10, 13, 29), our data demonstrate the superiority of CpG-B over CpG-A in stimulating B cells to proliferate and secrete Ab and proinflammatory cytokines. However, our results also highlight that CpG-A is not inert in B cells. Indeed, both CpG-A and CpG-B induce B cells to proliferate, secrete Abs and produce pro-inflammatory cytokines although as compared to CpG-A the responses to CpG-B were more rapid and of greater magnitude. Moreover, we show that the expression levels of a significant number of B cell surface proteins were similarly responsive to both CpG-A and CpG-B treatment.

A key novel finding reported here is the ability of CpG-A to induce B cells to upregulate type 1 IFN associated genes and to produce type 1 IFNs when CpG-A is conjugated to the cationic lipid DOTAP. We demonstrated that B cells responded to CpG-A-DOTAP *in vitro* but not to CpG alone by increasing expression of several type 1 IFN mRNAs, including IFN- $\alpha$ 2, - $\alpha$ 4, - $\alpha$ 5, and - $\beta$ 1, and secretion of IFN- $\beta$ 1. In addition, we provided evidence that CpG-A-DOTAP induced type-1-IFN *in vivo* and that B cells contributed to a significant portion of the type-1-IFN response *in vivo*, either directly or indirectly, as the IFN- $\beta$  response *in vivo* was significantly reduced in B-cell deficient as compared to WT mice. We also provided evidence that both TLR9-dependent and -independent mechanisms play a role in the B cell response to CpG-A. So far, at least two studies document TLR9-independent effects triggered when DCs and macrophages are stimulated with DOTAP-DNA complexes (30, 31). DOTAP, a cationic lipid, may fuse with the plasma membrane before internalization or endosomal membranes following internalization and release CpG-A into the cytosol. If so, various nucleic acid sensors (32) might be responsible for the observed TLR9-independent response

Another likely explanation for the observed TLR-9 independent effects is the modifications carried out in the synthesis of these synthetic ODNs. Previously non CpG ODNs with phosphorothioate backbones but not with phosphodiester backbones were shown to be capable of triggering intracellular signaling pathways and inducing interleukin synthesis (33, 34). It has also been reported that phosphorothioate modified synthetic ODN's may penetrate into cytoplasm and carry out various biological activities by binding to cytoplasmic proteins (35). Therefore the TLR-9 independent induction of type I interferons we observed here may also be the result of the enhanced bioactivity of synthetic CpG-A ODNs due to their phosphorothioate backbones.

In contrast, no detectable type 1 IFN was produced by B cells treated with CpG-B or CpG-B-DOTAP. Moreover, an analysis of the transcription of 80 genes associated with the expression or response to type 1 IFN and expression of proinflammatory cytokines showed that B cell treated with CpG-B or CpG-B-DOTAP not only fail to increase expression of type 1 IFN related genes but down regulate the expression of these genes as compared to untreated B cells.

These observations raise questions concerning the mechanism underlying the differential effect of CpG-A versus CpG-B and their DOTAP conjugates on B cells. Several studies in pDCs and conventional DCs provide insights into the cellular mechanisms that may contribute to this apparent dichotomy and suggest that TLR9 signaling is under spatiotemporal regulation. In pDCs CpG-A accumulates in early endosomes or LC3-positive phagosomes and triggers TLR-9 to signal for type 1 IFN synthesis (13, 36). In contrast, CpG-B rapidly traffics to late endosomes in pDCs and is inactive. Thus, intrinsic differences in CpG-A and CpG-B appear to restrict these in pDCs to either early endosomes for CpG-A and to late endosomes/lysosomes for CpG-B. Accumulation in early endosomes appears to be essential to trigger a type 1-IFN response. Indeed conjugation of CpG-B to DOTAP resulted in accumulation in early endosomes in pDC and a type 1-IFN response. In conventional DCs, CpG-A and CpG-B trafficked to late endosomes and triggered NK- $\kappa$ B-dependent inflammatory responses but not type 1 IFN responses. However, when CpG-A was conjugated to DOTAP, the CpG-A-DOTAP conjugate was retained in the early endosomes and signaled through TLR9 for a type 1 IFN response (13, 36). Thus, conjugation to DOTAP appeared to alter the trafficking of ODNs in pDCs and DCs and as a consequence altered the outcome of TLR9 ligation. One potential contributor to the differential responses to CpG-A versus CpG-B is the differences in the intracellular trafficking of CpG-A and CpG-B. Avalos *et al.* (10) provided evidence that CpG-A as compared to CpG-B was a poor TLR9 stimulant which might be explained in part by the observation that CpG-A and CpG-B accumulated in distinct intracellular compartments. However, when conjugated to immune complexes (ICs) CpG-A triggered B cells that expressed BCRs specific for ICs to proliferate comparably to CpG-B treated B cells. One explanation is that the BCR altered the intracellular trafficking of the bound CpG-A-ICs.

Here we showed that CpG-B was readily internalized and trafficked to LysoTracker-positive acidic compartments, whereas CpG-A accumulated in LysoTracker-negative compartments. We also tested the effect on B cells of conjugating CpGs to the cationic lipid, DOTAP. Our data revealed that CpG-A-DOTAP, like CpG-A, accumulated in LysoTracker-negative

compartments. However, CpG-A-DOTAP and CpG-A induced qualitatively different cytokine responses with only CpG-A-DOTAP inducing type 1 IFN secretion. Thus, although we did not observe a spatial change in the accumulation of CpG-A and CpG-A-DOTAP in B cells it is possible that the LysoTracker-negative compartments in which CpG-A and CpG-A-DOTAP resided were not identical. In contrast, CpG-B quickly accumulated in LysoTracker-positive compartments and accumulation was enhanced by conjugation to DOTAP. DOTAP might function in responses to CpG-B by facilitating the endosomal transport rate and/or by acting to prevent the degradation of CpG-B. Overall, considering the important role of endosomal pH in the maturation and the functioning of TLR9 (37, 38), the differences in the endosomal trafficking of the CpG-A and CpG-B are likely to contribute, at least in part, for the differences observed in the nature of B cells in response to these TLR9 ligands.

In conclusion, we provided evidence that both CpG-B and to a lesser extent CpG-A activate B cells to proliferate and secrete Abs and IL-6. However, CpG-A but not CpG-B induced type 1 IFN responses in B cells when incorporated into the cationic lipids. These results have important implications for the use of CpG-A and CpG-B as immunomodulators *in vivo*.

## Supplementary Material

Refer to Web version on PubMed Central for supplementary material.

## Acknowledgments

This study was supported by the Intramural Research Program of the National Institutes of Health, National Institute of Allergy and Infectious Diseases. MR and AC are funded by DBT junior research fellowship and IISER intramural funds respectively.

## References

1. Hemmi H, Takeuchi O, Kawai T, Kaisho T, Sato S, Sanjo H, Matsumoto M, Hoshino K, Wagner H, Takeda K, Akira S. A Toll-like receptor recognizes bacterial DNA. *Nature*. 2000; 408:740–745. [PubMed: 11130078]
2. Ashkar AA, Rosenthal KL. Toll-like receptor 9, CpG DNA and innate immunity. *Curr Mol Med*. 2002; 2:545–556. [PubMed: 12243247]
3. Kumagai Y, Takeuchi O, Akira S. TLR9 as a key receptor for the recognition of DNA. *Adv Drug Deliv Rev*. 2008; 60:795–804. [PubMed: 18262306]
4. Hua Z, Hou B. TLR signaling in B-cell development and activation. *Cellular & molecular immunology*. 2013; 10:103–106. [PubMed: 23241902]
5. DeFranco AL, Rookhuizen DC, Hou B. Contribution of Toll-like receptor signaling to germinal center antibody responses. *Immunol Rev*. 2012; 247:64–72. [PubMed: 22500832]
6. Rawlings DJ, Schwartz MA, Jackson SW, Meyer-Bahlburg A. Integration of B cell responses through Toll-like receptors and antigen receptors. *Nat Rev Immunol*. 2012; 12:282–294. [PubMed: 22421786]
7. Klinman DM, Barnhart KM, Conover J. CpG motifs as immune adjuvants. *Vaccine*. 1999; 17:19–25. [PubMed: 10078603]
8. Klinman DM, Conover J, Coban C. Repeated administration of synthetic oligodeoxynucleotides expressing CpG motifs provides long-term protection against bacterial infection. *Infect Immun*. 1999; 67:5658–5663. [PubMed: 10531213]
9. Klinman D, Shirota H, Tross D, Sato T, Klaschik S. Synthetic oligonucleotides as modulators of inflammation. *J Leukoc Biol*. 2008; 84:958–964. [PubMed: 18430787]

10. Avalos AM, Latz E, Mousseau B, Christensen SR, Shlomchik MJ, Lund F, Marshak-Rothstein A. Differential cytokine production and bystander activation of autoreactive B cells in response to CpG-A and CpG-B oligonucleotides. *J Immunol.* 2009; 183:6262–6268. [PubMed: 19864612]
11. Kerkmann M, Costa LT, Richter C, Rothenfusser S, Battiany J, Hornung V, Johnson J, Englert S, Ketterer T, Heckl W, Thalhammer S, Endres S, Hartmann G. Spontaneous formation of nucleic acid-based nanoparticles is responsible for high interferon-alpha induction by CpG-A in plasmacytoid dendritic cells. *J Biol Chem.* 2005; 280:8086–8093. [PubMed: 15591070]
12. Gursel I, Gursel M, Ishii KJ, Klinman DM. Sterically stabilized cationic liposomes improve the uptake and immunostimulatory activity of CpG oligonucleotides. *J Immunol.* 2001; 167:3324–3328. [PubMed: 11544321]
13. Honda K, Ohba Y, Yanai H, Negishi H, Mizutani T, Takaoka A, Taya C, Taniguchi T. Spatiotemporal regulation of MyD88-IRF-7 signalling for robust type-I interferon induction. *Nature.* 2005; 434:1035–1040. [PubMed: 15815647]
14. Scheu S, Dresing P, Locksley RM. Visualization of IFNbeta production by plasmacytoid versus conventional dendritic cells under specific stimulation conditions in vivo. *Proc Natl Acad Sci U S A.* 2008; 105:20416–20421. [PubMed: 19088190]
15. Kitamura D, Roes J, Kuhn R, Rajewsky K. A B cell-deficient mouse by targeted disruption of the membrane exon of the immunoglobulin mu chain gene. *Nature.* 1991; 350:423–426. [PubMed: 1901381]
16. Traba J, Miozzo P, Akkaya B, Pierce SK, Akkaya M. An Optimized Protocol to Analyze Glycolysis and Mitochondrial Respiration in Lymphocytes. *J Vis Exp.* 2016
17. Gordon EB, Hart GT, Tran TM, Waisberg M, Akkaya M, Skinner J, Zinocker S, Pena M, Yazew T, Qi CF, Miller LH, Pierce SK. Inhibiting the Mammalian target of rapamycin blocks the development of experimental cerebral malaria. *mBio.* 2015; 6:e00725. [PubMed: 26037126]
18. Kamenyeva O, Boullaran C, Kabat J, Cheung GY, Cicala C, Yeh AJ, Chan JL, Periasamy S, Otto M, Kehrl JH. Neutrophil recruitment to lymph nodes limits local humoral response to *Staphylococcus aureus*. *PLoS Pathog.* 2015; 11:e1004827. [PubMed: 25884622]
19. Akkaya B, Miozzo P, Holstein AH, Shevach EM, Pierce SK, Akkaya M. A Simple, Versatile Antibody-Based Barcoding Method for Flow Cytometry. *J Immunol.* 2016; 197:2027–2038. [PubMed: 27439517]
20. Doyle SE, O'Connell RM, Miranda GA, Vaidya SA, Chow EK, Liu PT, Suzuki S, Suzuki N, Modlin RL, Yeh WC, Lane TF, Cheng G. Toll-like receptors induce a phagocytic gene program through p38. *J Exp Med.* 2004; 199:81–90. [PubMed: 14699082]
21. Sester DP, Brion K, Trieu A, Goodridge HS, Roberts TL, Dunn J, Hume DA, Stacey KJ, Sweet MJ. CpG DNA activates survival in murine macrophages through TLR9 and the phosphatidylinositol 3-kinase-Akt pathway. *J Immunol.* 2006; 177:4473–4480. [PubMed: 16982883]
22. Barr TA, Shen P, Brown S, Lampropoulou V, Roch T, Lawrie S, Fan B, O'Connor RA, Anderton SM, Bar-Or A, Fillatreau S, Gray D. B cell depletion therapy ameliorates autoimmune disease through ablation of IL-6-producing B cells. *J Exp Med.* 2012; 209:1001–1010. [PubMed: 22547654]
23. Kohm AP, Mozaffarian A, Sanders VM. B cell receptor- and beta 2-adrenergic receptor-induced regulation of B7-2 (CD86) expression in B cells. *J Immunol.* 2002; 168:6314–6322. [PubMed: 12055247]
24. Prazma CM, Yazawa N, Fujimoto Y, Fujimoto M, Tedder TF. CD83 expression is a sensitive marker of activation required for B cell and CD4+ T cell longevity in vivo. *J Immunol.* 2007; 179:4550–4562. [PubMed: 17878352]
25. Keir ME, Butte MJ, Freeman GJ, Sharpe AH. PD-1 and its ligands in tolerance and immunity. *Annu Rev Immunol.* 2008; 26:677–704. [PubMed: 18173375]
26. Taniguchi T, Ogasawara K, Takaoka A, Tanaka N. IRF family of transcription factors as regulators of host defense. *Annu Rev Immunol.* 2001; 19:623–655. [PubMed: 11244049]
27. Kato H, Fujita T. RIG-I-like receptors and autoimmune diseases. *Curr Opin Immunol.* 2015; 37:40–45. [PubMed: 26530735]
28. Schoggins JW, Rice CM. Interferon-stimulated genes and their antiviral effector functions. *Current opinion in virology.* 2011; 1:519–525. [PubMed: 22328912]

29. Rothenfusser S, Hornung V, Ayyoub M, Britsch S, Towarowski A, Krug A, Sarris A, Lubenow N, Speiser D, Endres S, Hartmann G. CpG-A and CpG-B oligonucleotides differentially enhance human peptide-specific primary and memory CD8+ T-cell responses in vitro. *Blood*. 2004; 103:2162–2169. [PubMed: 14630815]
30. Yasuda K, Yu P, Kirschning CJ, Schlatter B, Schmitz F, Heit A, Bauer S, Hochrein H, Wagner H. Endosomal translocation of vertebrate DNA activates dendritic cells via TLR9-dependent and -independent pathways. *J Immunol*. 2005; 174:6129–6136. [PubMed: 15879108]
31. Yasuda K, Ogawa Y, Yamane I, Nishikawa M, Takakura Y. Macrophage activation by a DNA/cationic liposome complex requires endosomal acidification and TLR9-dependent and -independent pathways. *J Leukoc Biol*. 2005; 77:71–79. [PubMed: 15496451]
32. Keating SE, Baran M, Bowie AG. Cytosolic DNA sensors regulating type I interferon induction. *Trends Immunol*. 2011; 32:574–581. [PubMed: 21940216]
33. Bartz H, Mendoza Y, Gebker M, Fischborn T, Heeg K, Dalpke A. Poly-guanosine strings improve cellular uptake and stimulatory activity of phosphodiester CpG oligonucleotides in human leukocytes. *Vaccine*. 2004; 23:148–155. [PubMed: 15531031]
34. Bekeredjian-Ding I, Doster A, Schiller M, Heyder P, Lorenz HM, Schraven B, Bommhardt U, Heeg K. TLR9-activating DNA up-regulates ZAP70 via sustained PKB induction in IgM+ B cells. *J Immunol*. 2008; 181:8267–8277. [PubMed: 19050243]
35. Ziegler S, Eberle ME, Wolfle SJ, Heeg K, Bekeredjian-Ding I. Bifunctional oligodeoxynucleotide/antagomiR constructs: evaluation of a new tool for microRNA silencing. *Nucleic Acid Ther*. 2013; 23:427–434. [PubMed: 24236889]
36. Sasai M, Linehan MM, Iwasaki A. Bifurcation of Toll-like receptor 9 signaling by adaptor protein 3. *Science*. 2010; 329:1530–1534. [PubMed: 20847273]
37. Park B, Brinkmann MM, Spooner E, Lee CC, Kim YM, Ploegh HL. Proteolytic cleavage in an endolysosomal compartment is required for activation of Toll-like receptor 9. *Nat Immunol*. 2008; 9:1407–1414. [PubMed: 18931679]
38. Rutz M, Metzger J, Gellert T, Lippa P, Lipford GB, Wagner H, Bauer S. Toll-like receptor 9 binds single-stranded CpG-DNA in a sequence- and pH-dependent manner. *Eur J Immunol*. 2004; 34:2541–2550. [PubMed: 15307186]

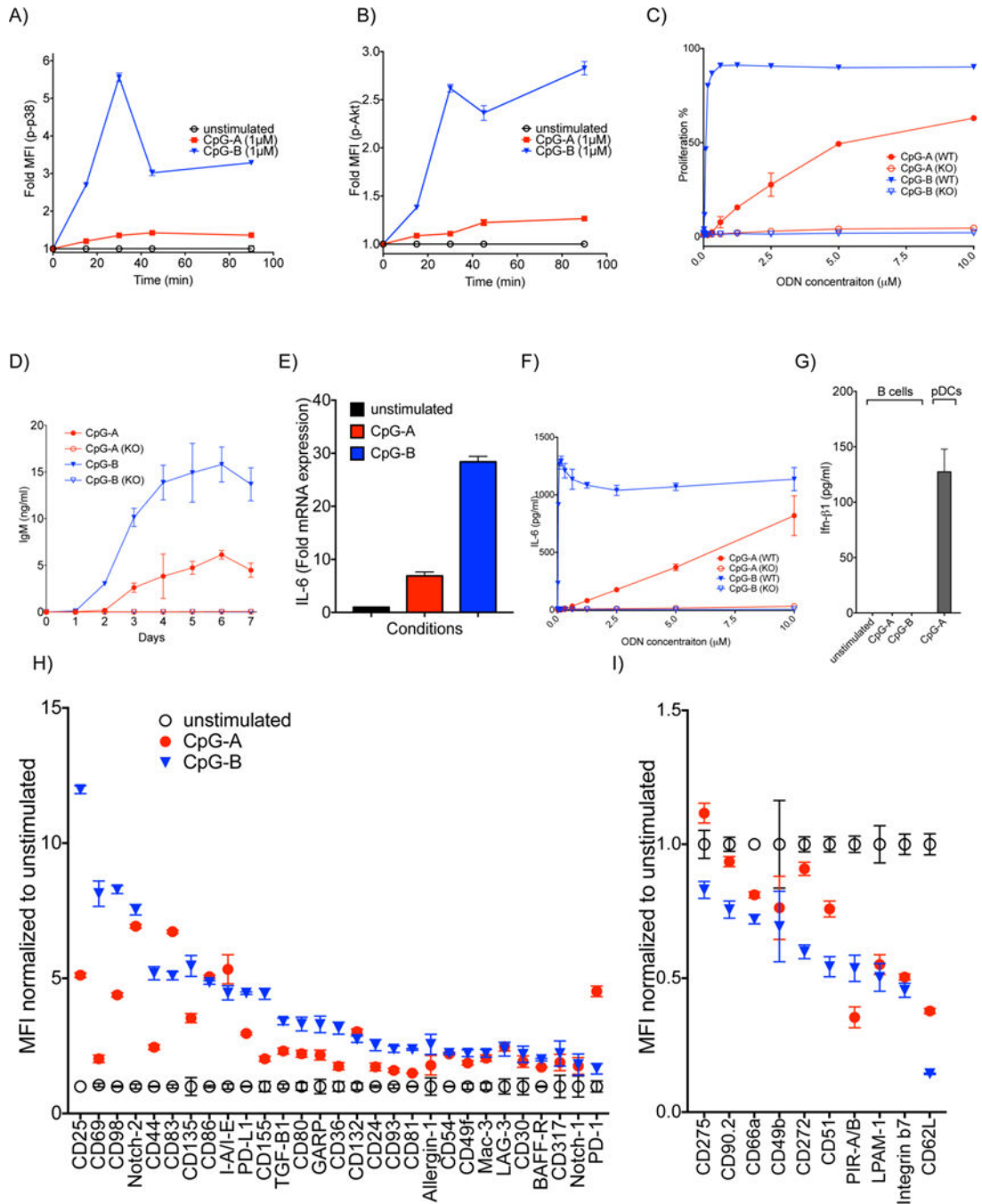


**Figure 1.**

The effect of CpG-A and CpG-B on B cells *in vitro*. A-B) B cells were treated with 1 μM CpG-A or CpG-B for increasing lengths of time. The fold change of phosphorylation of kinases in stimulated versus unstimulated B cells was determined by phosphoflow. Shown are the fold changes in MFI for: A) phospho-p38 and B) phospho-Akt. C) B cells purified from spleens of either WT or TLR9 KO mice were incubated with increasing concentrations of CpG-A or CpG-B for 48 h. The percentage of B cells that proliferated at least once was determined by flow cytometry. D) B cells purified from WT or TLR9 KO mice were



incubated with 2  $\mu$ M CpG-A or CpG-B. Supernatants were collected daily for 7 days and levels of secreted IgM were measured by ELISA. E) Purified mouse B cells were stimulated with 5  $\mu$ M CpG-A or CpG-B for 90 min and the fold changes in the levels of mRNA encoding IL-6 compared to the unstimulated B cells were determined by qPCR. F) B cells were purified and treated as in (C) and the levels of IL-6 in the supernatants was measured 18 h later. G) Purified B cells or as a positive control, pDCs isolated from spleens, were treated with 5  $\mu$ M CpG-A or CpG-B for 16 h and the levels of IFN- $\beta$  in the supernatants were measured by ELISA. H,I) Purified B cells were treated with 2  $\mu$ M CpG-A or CpG-B for 24 h. Cells were barcoded, pooled and stained with PE- conjugated Abs specific for the surface markers shown. H) Fold up-regulation or I) down-regulation in the MFI of markers compared to untreated cells are shown. Data represent at least three independent experiments each of which contains three replicates.

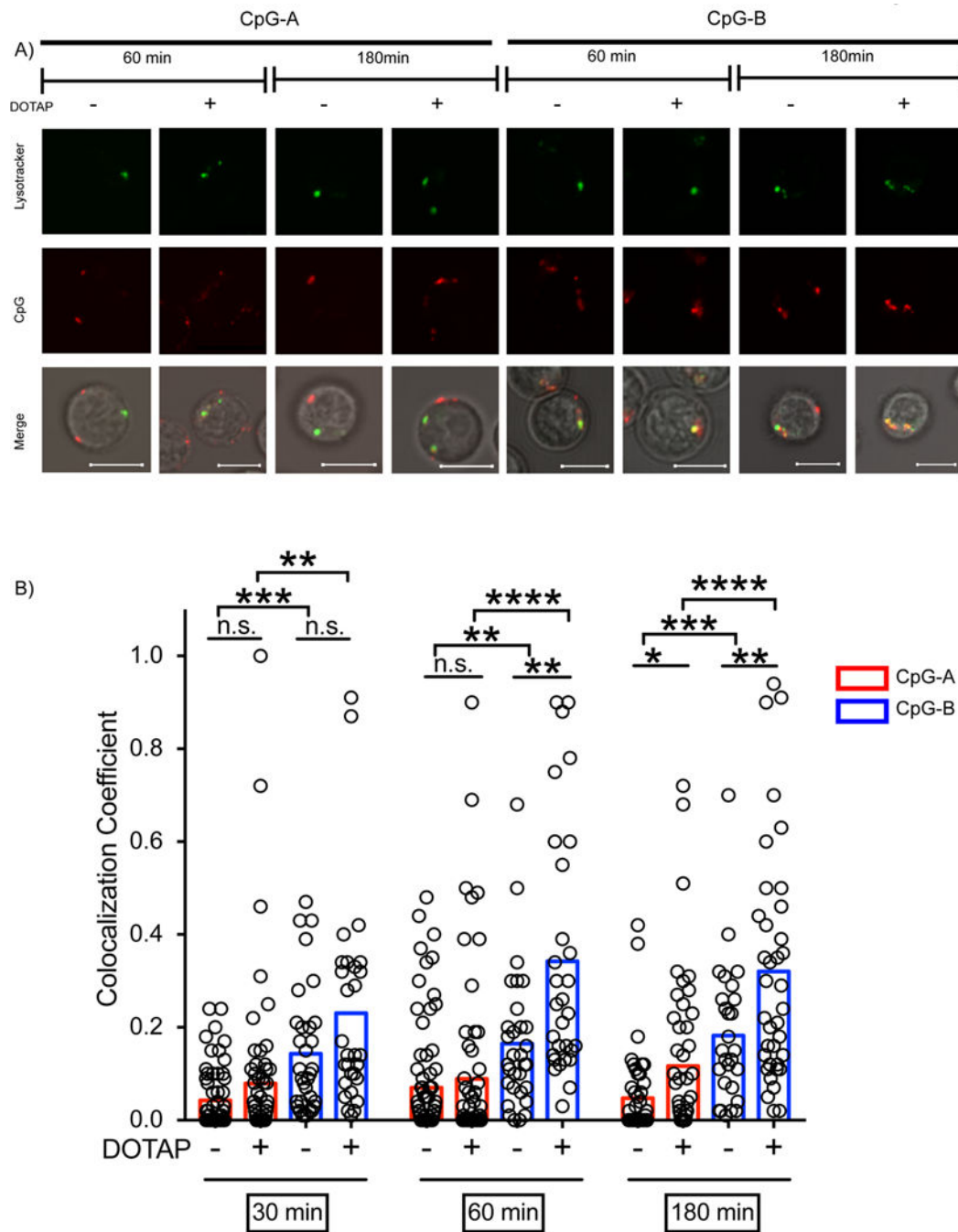


**Figure 2.** The intracellular trafficking of CpG-A and CpG-B and their DOTAP conjugates. A) Purified mouse B cells were incubated with 1 μM Cy-3-CpG-A or 1 μM Cy-5-CpG-B or their DOTAP conjugates (1:3 w/w ratio) for 30, 60 or 180 min, stained with LysoTracker and imaged by confocal microscopy. Shown are representative images of B cells showing localization of the CpG-ODNs, LysoTracker and the merged images at the 60 and 180 min time points. Scale bars represent 5 μm. B) The colocalization of CpG-A or CpG-B with LysoTracker was quantified. (n = 30). Each symbol represents one cell. Results are representative of more than

four independent experiments. ( $P > 0.05 = \text{ns}$ ;  $0.01 < P < 0.05 = *$ ;  $0.001 < P < 0.01 = **$ ;  
 $0.0001 < P < 0.001 = ***$ ;  $P < 0.0001 = ****$ )

Author Manuscript

Author Manuscript

Author Manuscript

Author Manuscript

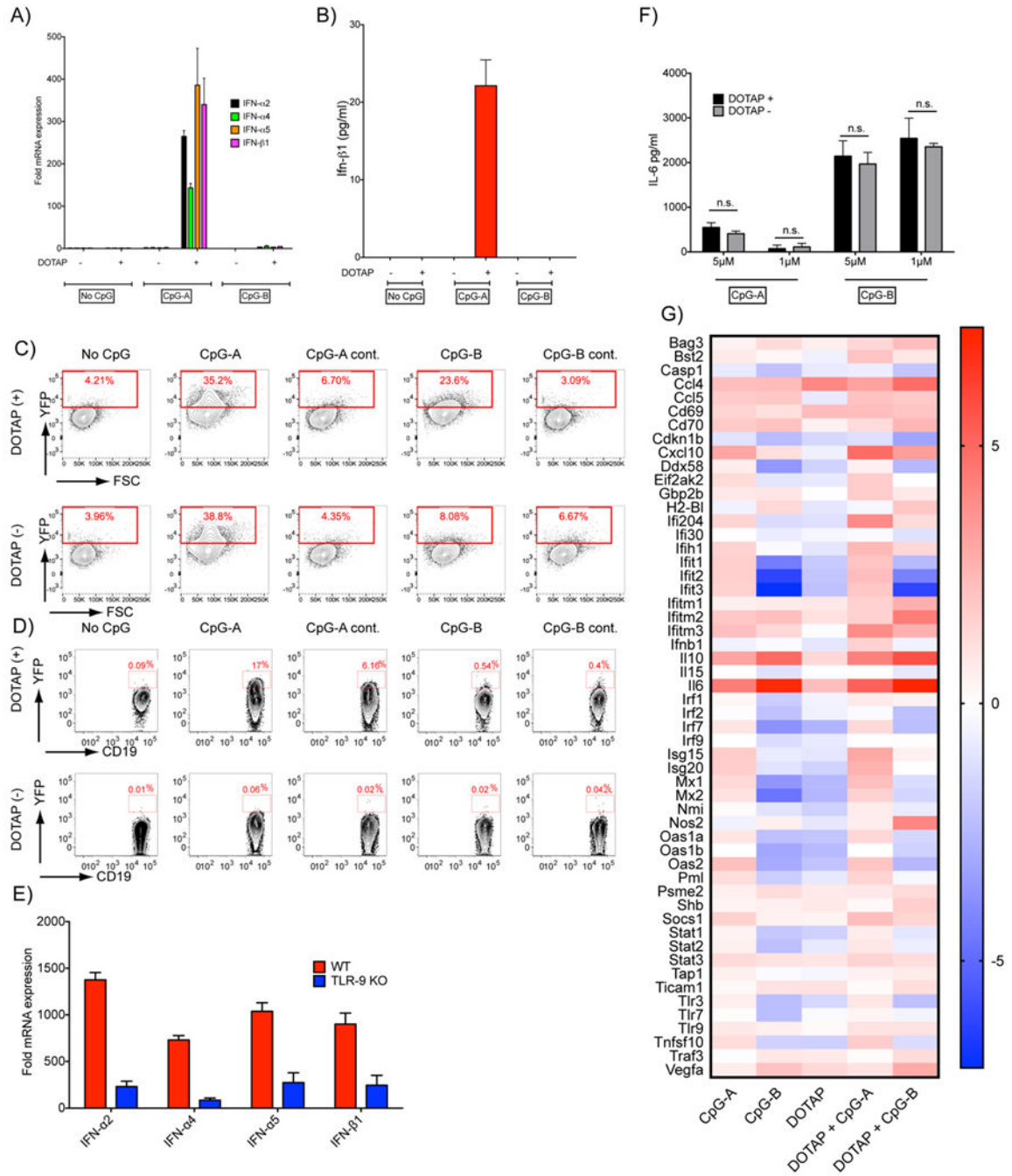


**Figure 3.** Stimulation of B cells with CpG-A-DOTAP induces a type-1 IFN response. A) Purified B cells were stimulated with 5 μM CpG-A or CpG-B or their DOTAP conjugates. Cells were cultured for 90 min and the fold changes in the expression of type-1 IFN genes compared to unstimulated B cells was determined. B) Purified B cells were stimulated as described in (A) and cultured for 16 h and IFN-β was measured in the culture supernatants. C) pDCs generated from the bone marrow cells of IFN-β YFP mice D) B cells purified from the spleens of the same strain were treated with CpG-A, CpG-B or control (GpC) ODNs with or

without DOTAP for 18 h and in the fold change in expression of YFP determined by flow cytometry. Representative flow cytometry plots are shown. Data represent more than five independent experiments. E) B cells purified from either WT or TLR9 KO mice were stimulated with DOTAP-CpGA for 90 min. The fold change in the mRNA expression of type 1 IFN genes compared to their respective unstimulated controls are shown. F) Purified B cells were treated with CpG-A or CpG-B on their DOTAP conjugates at 1 or 5  $\mu$ M. G) Purified B cells were stimulated with 2  $\mu$ M CpG-A or CpG-B with or without DOTAP (1:3 ratio) for 6 h. The expression of a preselected set of genes were measured using a qPCR assay (n=3). Heat map shows the average change for each gene in stimulated relative to the unstimulated control in log<sub>2</sub> scale.

Author Manuscript

Author Manuscript

Author Manuscript

Author Manuscript

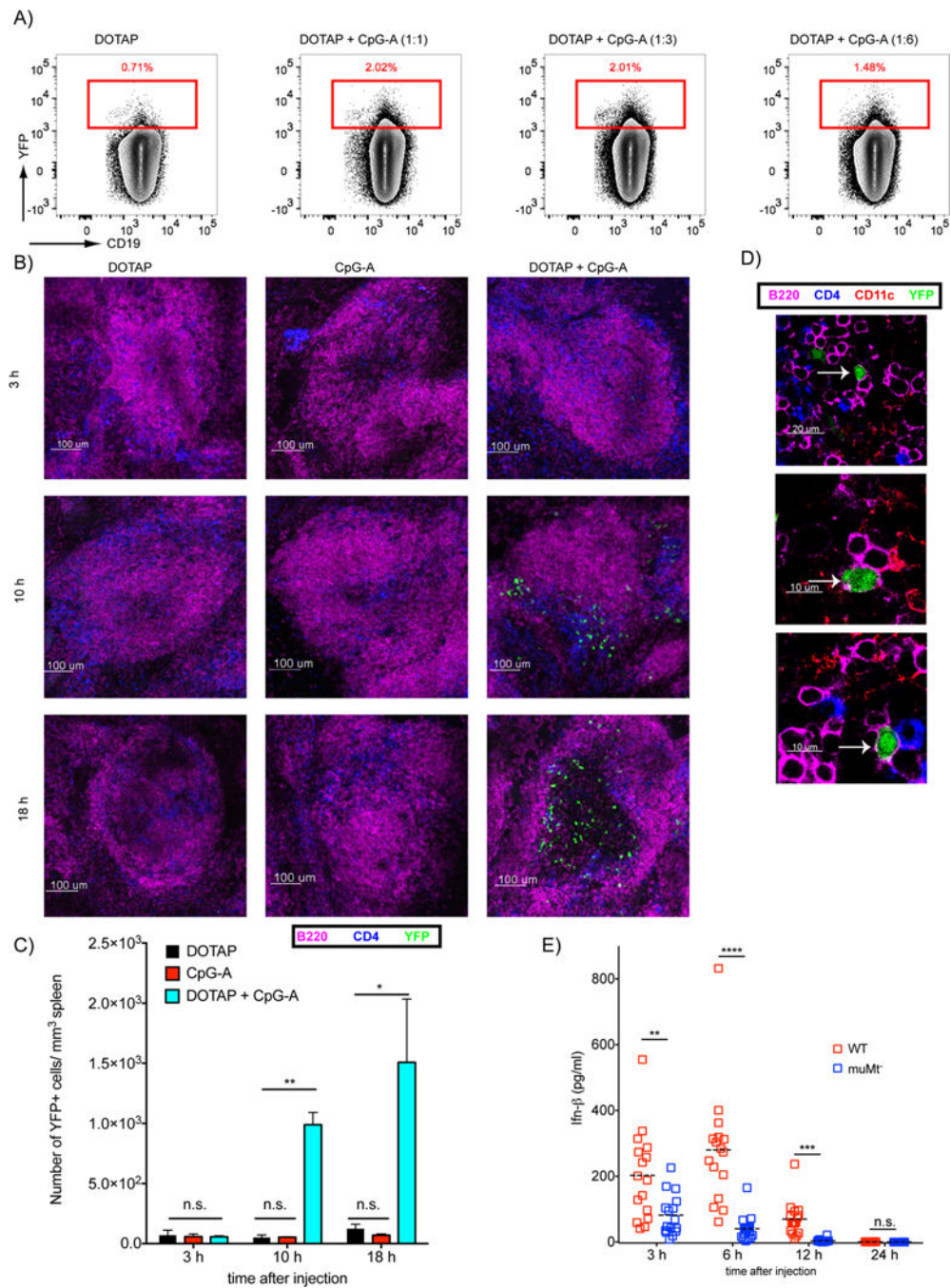


**Figure 4.**

B cells produce type 1 IFN in response to CpG-A-DOTAP *in vivo*. A) IFN- $\beta$ -YFP mice were injected i.v. with HBS supplemented with either 45 $\mu$ g/mouse DOTAP alone or conjugated with 45, 15 or 7.5  $\mu$ g/mouse CpG-A. Spleens were collected 18h post injection and analyzed by flow cytometry. Flow cytometry plots show the YFP fluorescence in the B cell gate. B) IFN- $\beta$  YFP mice were injected with CpG-A (25  $\mu$ g/mouse), DOTAP (75  $\mu$ g/mouse) or CpG-A-DOTAP intravenously and spleens were harvested at 3, 10, 18 h post injection. Spleens were immediately embedded in agarose, sectioned, stained for surface

markers and imaged by confocal microscopy. Representative images showing B cells (Magenta), T cells (Blue) and YFP signal (Green) are shown. C) YFP cells (B) were quantified for each time point from data collected in three independent experiments. D) Representative images showing YFP in B cells (B220<sup>+</sup> CD11c<sup>-</sup>). E) WT and muMt<sup>-</sup> mice were injected with CpG-A (25 µg/mouse) combined with DOTAP (75 µg/mouse) intravenously. Blood samples were collected 3 h, 6 h, 12 h and 24 h post injection and serum levels of IFN-β were measured by ELISA. Shown are the combined IFN levels from three independent experiments with a total of 18 mice per experimental time point. Each symbol represents one mouse. (P>0.05 = ns; 0.01 <P 0.05 = \*; 0.001 <P 0.01 = \*\*; 0.0001 <P 0.001 = \*\*\*; <P 0.0001 = \*\*\*\*)

Author Manuscript

Author Manuscript

Author Manuscript

Author Manuscript